10th International Winds Workshop, Tokyo, Japan 22-26 February 2010

Investigating Height Assignment Type Errors in the NCEP Global Forecast System

James Jung[1,5], John Le Marshall[2], Jaime Daniels[3], Lars Peter Riishojgaard[4,5]

[1]Cooperative Institute for Meteorological Satellite Studies, Madison, WI

[2]Centre for Australian Weather and Climate Research, Melbourne, Australia

[3]NOAA/SESDIS, Center for Satellite Applications and Research, Camp Springs, MD

[4]Uninversity of Maryland Baltimore County, Baltimore, MD

[5]Joint Center for Satellite Data Assimilation, Camp Springs, MD

Abstract

Within the Numerical Weather Prediction community the observation errors for Atmospheric Motion Vectors (AMV) are assigned by the image type (infrared, visible, water vapor) and/or tracking feature (cloud top, clear air). We are investigating a new approach which involves basing the observation error on AMV height assignment type. We will be presenting AMV statistics for the various height assignment types with respect to the National Centers for Environmental Prediction (NCEP) Global Forecast System (GFS) background. We will also be discussing potential quality control and thinning procedures.

INTRODUCTION

Since the seventies, wind vectors have been estimated from space using sequential imagery form geostationary satellites. These Atmospheric Motion Vectors (AMVs) provide information about atmospheric circulations and are especially valuable for weather forecast models in regions where other information is sparse, as over oceans. AMVs continue to be troubled by inaccurate height assignment of the cloud tracers, especially in thin clouds that are semi-transparent in the infrared window wavelengths. Over the years several height assignment techniques have been developed, each with their own assumptions and error characteristics.

The purpose of this study is to quantify the errors associated with each of the AMV height assignment techniques used operationally at NOAA/NESDIS. Once quantified, this information can be used to improve the assimilation techniques and potentially improve the impact and forecast skill AMVs have in numerical weather prediction models.

HEIGHT ASSIGNMENT TYPES

Currently, heights are assigned by one of five techniques when the appropriate spectral radiance measurements are available: infrared window (WIN), CO_2 ratio (CO_2), water vapor intercept (H_2O), histogram (HIST) and cloud base. Each wind observation has height assignments from most, if not all, height assignment techniques. The National Environmental Satellite, Data, and Information Service (NESDIS) has ordered the height assignment types according to the performance of each height assignment technique as determined by AMV/rawindonde comparison statistics. The ranking of height assignment techniques that NESDIS has chosen is CO_2, H_2O, and WIN. If a higher ranking method fails for any reason the next ranking height assignment method is chosen for the observation height. The re-assigned heights from the NESDIS auto-editor were not used in these experiments.

In semitransparent or small subpixel clouds, the CO_2 technique uses the ratio of radiances from different layers of the atmosphere to infer the correct cloud height. The technique calculates the spectral radiative transfer in an atmosphere with a single height cloud layer. It accounts for any semi-transparency of the cloud. The difference in clear and cloudy radiances is measured for the infrared window and the CO_2 channel(s). The clear radiances are calculated from a short term NCEP GFS model forecast profile. Since the emissivity of ice clouds and the cloud fractions for the window and CO_2 channels are roughly the same, the cloud top pressure of the cloud within the field of view can be specified. This technique is explained in Menzel et al. (1983). The CO_2 technique fails when the difference between the observed and clear radiances in any of the channels is less than the instrument noise. This happens for low broken cloud or very thin cirrus. Another difficulty occurs in two cloud layer situations. In this case the CO_2 technique will produce a cloud layer somewhere in between the actual two cloud layers.

In the H_2O technique, radiances influenced by upper-tropospheric moisture and infrared window radiances are measured for several pixels viewing different cloud amounts, and their linear relationship is used to extrapolate the correct cloud height. Thus, a plot of H_2O radiances versus IRW radiances in a scene of varying cloud amount will be nearly linear. These radiance measurements are used in conjunction with radiative transfer calculations for both spectral channels derived from a short term NCEP GFS forecast model temperature and moisture profile. The intersection of the measured and calculated radiances will occur at the clear-sky and opaque cloud radiances. The cloud-top temperature is extracted from the cloud-clear radiance intersection. The details of this technique are similar to Szejwach (1982) and are explained in Nieman et al. (1993). Since the H_2O radiances are primarily emanating from the upper troposphere, height determinations below 600 hPa are rejected.

The histogram technique is similar to the infrared window technique, but is applied to water vapor brightness temperatures to assign heights to water vapor winds. If the target scene is deemed to be dominated by clouds, then the average of the coldest 20% of the water vapor brightness temperatures in the histogram is computed and compared to a short-term NCEP GFS forecast temperature profile to determine the cloud height. If the target scene is dominated by clear-sky conditions, then the average water vapor brightness temperatures from a 5x5 scene of pixels centered over the central pixel of the target scene are computed. The average clear-sky water vapor brightness temperature value is then compared to a short-term NCEP GFS forecast temperature profile to determine the height of the clear-sky water vapor wind.

The WIN technique compares measured brightness temperatures to forecast temperature profiles and thus infers opaque cloud levels. The technique uses the average of the coldest 20% of the infrared window channel brightness temperatures in the target scene and compares it to a short term NCEP GFS forecast temperature profile to determine the cloud height. For an opaque cloud this level is a good representation of the level of the cloud. The window channel estimate is used mostly for low clouds (below 600 hPa) and when other techniques experience problems.

A cloud base height technique (LeMarshall et al, 1994) is used to infer the height of low level clouds at their base. A histogram is derived from the brightness temperatures within the target scene. Determination of the cloud temperatures are then obtained by fitting Hermite polynomials to smooth the histograms containing cloud top and surface temperature. The portion of the histogram of cloud top allows an estimation of cloud base temperature from the Hermite polynomials. The cloud base temperature is then compared to a short term NCEP GFS model temperature profile to determine cloud base height. Heights assigned to cloud base were not part of this data set.

DEFINITION OF STATISTICS USED

The traditional assessment of the accuracy of cloud-motion winds is accomplished by comparison with collocated rawinsondes (Hayden and Nieman, 1996) and comparisons to a forecast model. The statistics used are basically the same, substituting the rawinsonde for the forecast model. For this paper we will be using the NCEP GFS 6 hour forecast. We are presenting statistics for wind speed as outlined in Nieman et al. (1997) and direction.

Speed

The vector difference (VD) between an individual wind report (i) and the forecast model (m) used for verification is given by:

$$(VD) = \sqrt{\left(U_i - U_m\right)^2 + \left(V_i - V_m\right)^2}$$

The speed bias is given by:

$$(BIAS) = \frac{1}{N}\sum_{i,m=1}^{N}\left(\sqrt{U_i^2 + V_i^2} - \sqrt{U_m^2 + V_m^2}\right)$$

The mean vector difference (MVD) is:

$$(MVD) = \frac{1}{N}\sum_{i=1}^{N}\left(VD\right)_i$$

The standard deviation about the mean vector difference (SD) is:

$$(SD) = \sqrt{\frac{1}{N}\sum_{i=1}^{N}\left[\left(VD_i\right) - \left(MVD\right)\right]^2}$$

The root mean square error (RMSE) is the square root of the sum of he squares of the mean vector difference and the standard deviation about the mean vector difference:

$$(RMSE) = \sqrt{\left(MVD\right)^2 + \left(SD\right)^2}$$

The normalized RMSE (NRMSE) is the root mean square error divided by the model average wind speed:

$$(NRMSE) = {(RMSE)}\Big/{Model\_wind\_speed}$$

Direction

The method for deriving vector $\vec{C}$ is in the Appendix. The directional root mean square error (DRMSE) is given by:

$$(DRMSE) = \sqrt{\frac{1}{N-1}\sum_{i=1}^{N}\vec{C}^{2}}$$

The directional bias (DBIAS) is given by:

$$(DBIAS) = \frac{1}{N}\sum_{i=1}^{N}\vec{C}$$

HEIGHT ASSIGNMENT STATISTICS

We have stratified the statistics by satellite and tracking image type. The water vapor channels are different on the two current Geostationary Operational Environmental Satellites (GOES). Thus, GOES-11 and GOES-12 have different error characteristics. GOES-12 also has a CO_2 channel allowing for the use of the CO_2 technique. Although the tracking methods are the same for the water vapor image and the infrared window image, the error characteristics of the height assignments are very different.

Twenty days in July and December (40 days total, 160 assimilation cycles) were used to derive these statistics. Since the statistics were similar for both seasons, the two datasets were merged. The values for each height assignment type were divided into 50 hPa levels. A level must have at least 100 samples to be plotted.

The statistics were also stratified into three latitude bands. The Northern Hemisphere included the region between 60^{o}N to 20^{o}N. The Tropical Region included 20^{o}N to 20^{o}S. The Southern Hemisphere included 20^{o}S to 60^{o}S.

Tracking using Water Vapor Images

The height assignment error statistics of normalized MVD RMSE and bias by pressure level for the water vapor image cloud top tracking technique applied to GOES-11 imager data are shown in Figure 1. In general, the CO_2, H_2O, and HIST technique RMSEs are consistent with each other. They show errors of around 0.5 except near the tropopause. The bias shows more inconsistency with the best being the H_2O technique. Most NWP centers use only those winds between the tropopause and 500 hPa. For the water vapor images, the WIN technique is not used for height assignment.

The height assignment error statistics of directional RMSE and bias for the water vapor image cloud top tracking technique applied to GOES-12 imager data are shown in Figure 2. In general, the CO_2, H_2O, and HIST techniques are again consistent with each other. Most winds have a directional RMSE of about 20^{o} and a bias of less than 5^{o} in the region used by most NWP centers (tropopause to 500 hPa). As mentioned earlier the WIN technique is not used as a height assignment type for the water vapor images.

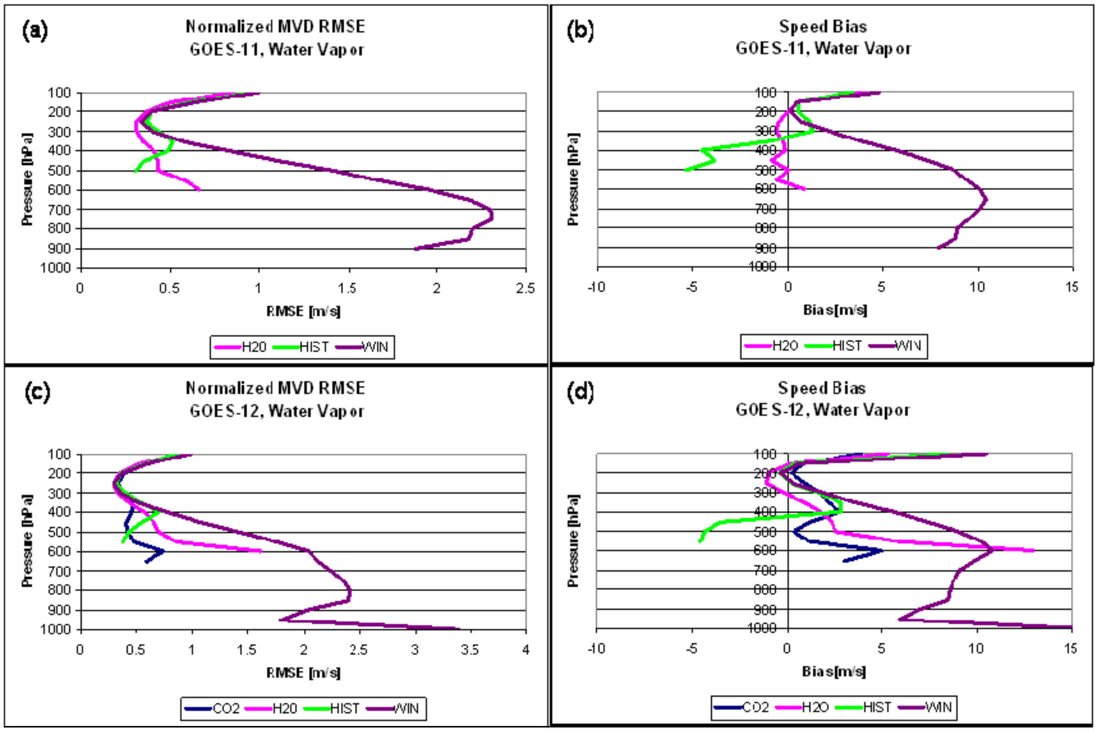

Figure 1: **Normalized MVD RMSE and speed bias vs pressure for the various height assignment types of cloud drift winds derived from the water vapor image. The top panels (a and b) are from GOES-11, the bottom panels (c and d) are from GOES-12.**

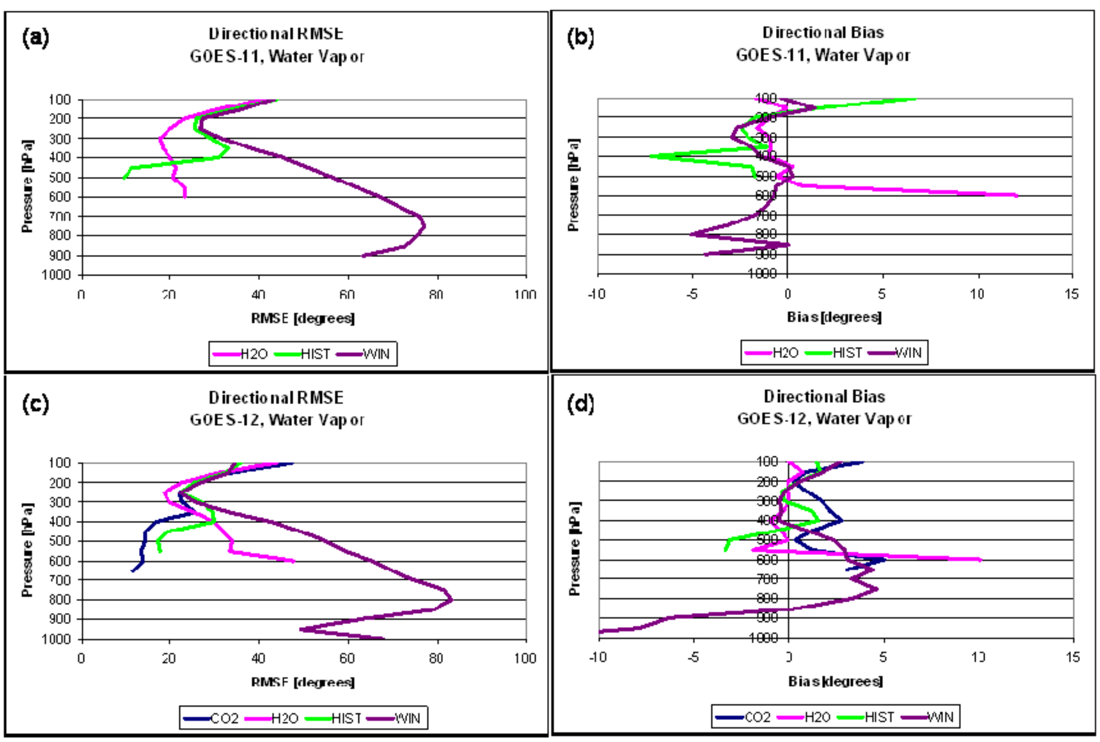

Figure 2: **Directional RMSE and bias vs pressure for the various height assignment types of cloud drift winds derived from the water vapor image. The top panels (a and b) are from GOES-11, the bottom panels (c and d) are from GOES-12.**

Tracking using Infrared Images

The height assignment error statistics of normalized MVD RMSE and bias by pressure level for the infrared window image cloud top tracking technique applied to GOES-12 imager data are shown in Figure 3. In contrast to the water vapor image, the infrared window image height assignment techniques show little consistency with each other. In general, the WIN technique has the least error and bias from the tropopause to around 400 hPa. Typically, the CO_2 and H_2O techniques are considered superior in this region. The CO_2 technique shows the least error in the lower levels but the sample size is small due to only using the CO_2 technique only for cloud top temperatures lower than 273K. The winds generated from the infrared window images do not use the HIST technique.

Similar error statistics are observed in the directional RMSE as with the normalized MVD RMSE and are shown in Figure 4. The directional bias in the H_2O and HIST techniques for GOES-11 are better than those observed for GOES-12. Again, the HIST technique is not a height assignment option for the infrared window images but is shown for completeness.

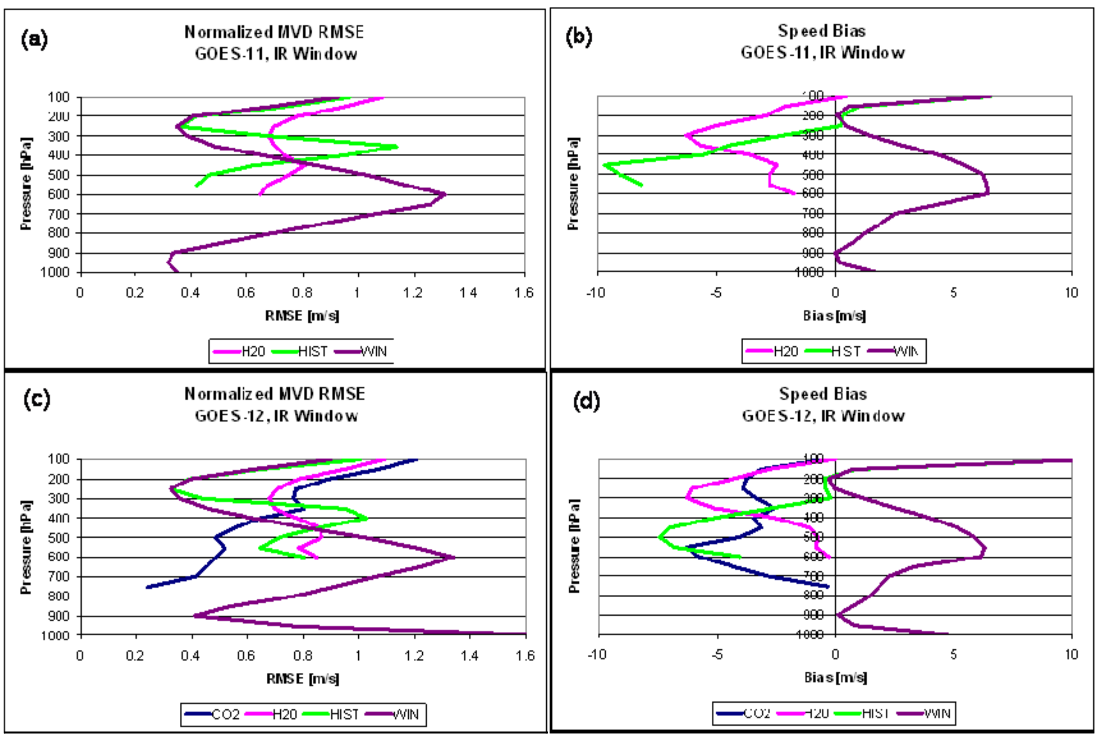

Figure 3: **Normalized MVD RMSE and speed bias vs pressure for the various height assignment types of cloud drift winds derived from the infrared window image. The top panels (a and b) are from GOES-11, the bottom panels (c and d) are from GOES-12.**

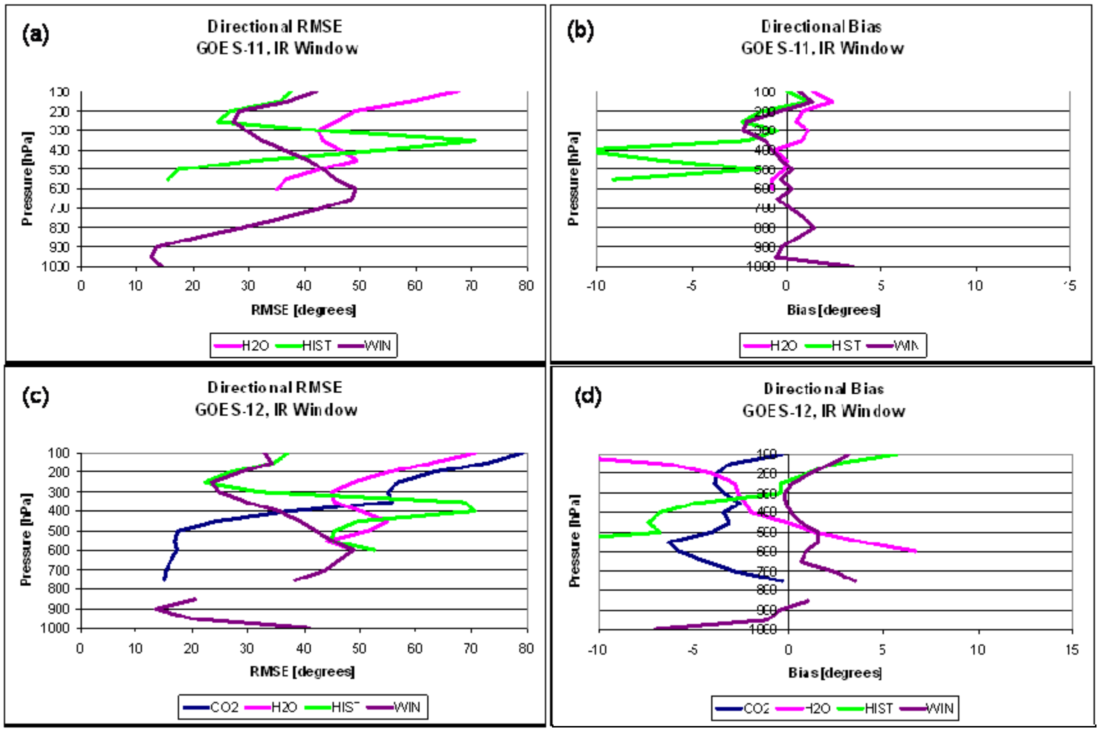

Figure 4: **Directional RMSE and bias vs pressure for the various height assignment types of cloud drift winds derived from the infrared window image. The top panels (a and b) are from GOES-11, the bottom panels (c and d) are from GOES-12.**

Latitudinal Differences

Stratifying the H_2O technique by latitude bands also shows some interesting results. The Northern and Southern Hemisphere statistics for normalized MVD RMSE and speed bias are very similar when using the water vapor image as shown in Figure 5. The statistics for the tropical region are consistently worse. We speculate this is a model issue as the tracking and height assignment technique do not have a latitudinal dependence.

The normalized MVD RMSEs for the infrared window based on latitude are consistent with both the results from the water vapor image (figure 5) and previous differences seen between the water vapor image and infrared window (figures 1 and 3). The Northern and Southern Hemisphere RMSE values are similar with the tropical region errors being greatest. Also, the infrared window errors are greater than those observed from the water vapor image. The speed bias characteristics in the three latitude bands are considerably different. The Southern Hemisphere has a large slow bias where as the tropical region is closest to zero bias. We suspect that there is also a model component to the bias.

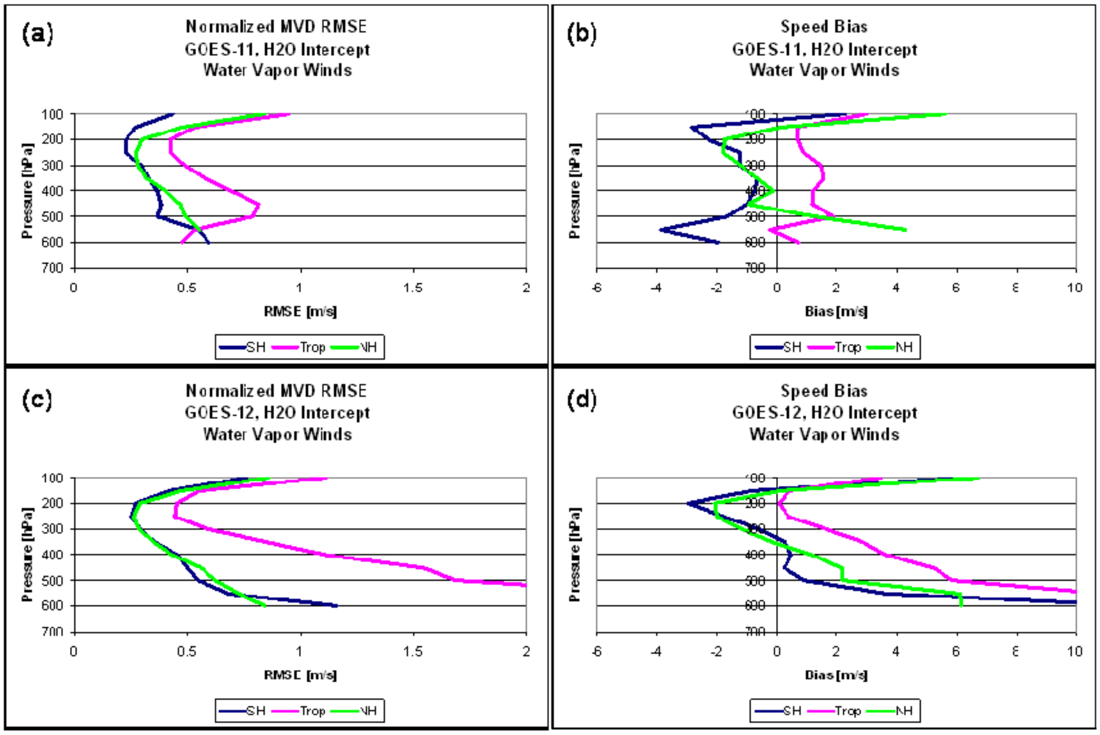

Figure 5: **Normalized MVD RMSE and speed bias vs pressure for the H2O height assignment technique in the Southern Hemisphere, Tropics, and Northern Hemisphere of cloud drift winds derived from the water vapor image. The top panels (a and b) are from GOES-11, the bottom panels (c and d) are from GOES-12.**

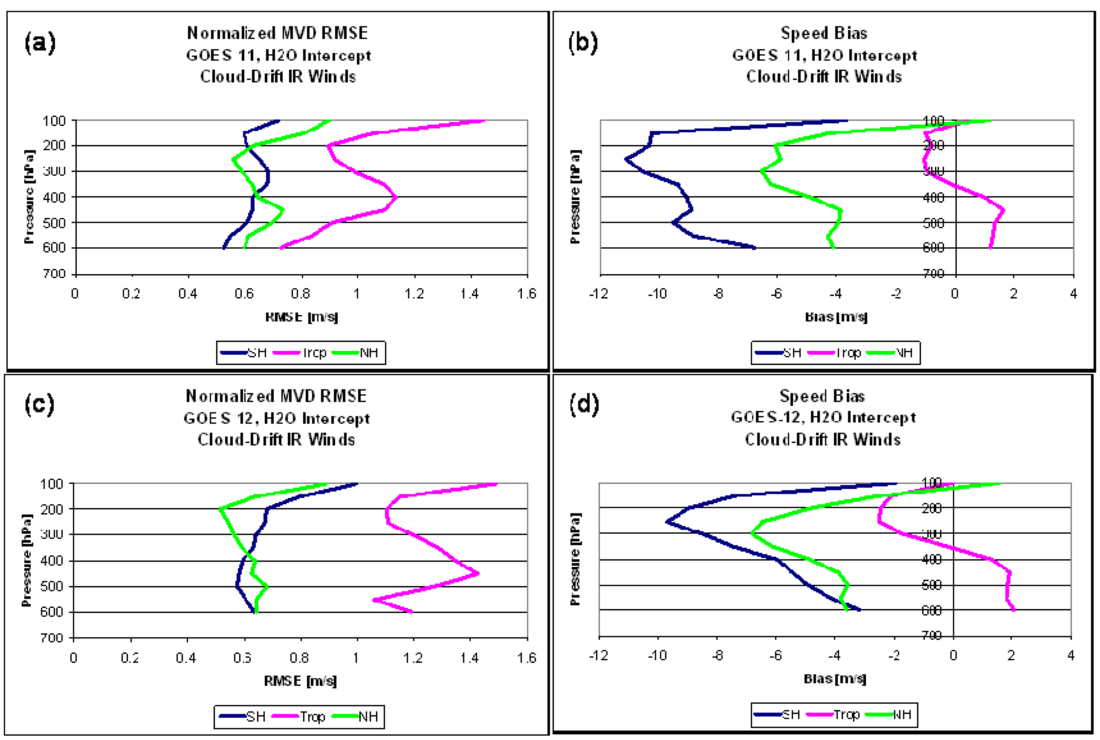

Figure 6: **Normalized MVD RMSE and speed bias vs pressure for the H2O height assignment technique in the Southern Hemisphere, Tropics, and Northern Hemisphere of cloud drift winds derived from the infrared window image. The top panels (a and b) are from GOES-11, the bottom panels (c and d) are from GOES-12.**

FUTURE PLANS

NCEP has several modifications planned for the satellite winds assimilation routines within their Gridpoint Statistical Interpolation (GSI) system which are also summarized in Su et al. 2010. Some of these modifications will include having the height assignment technique information available within the GSI and developing new quality control procedures based on the height assignment and directional differences.

Work is also continuing within NESDIS and the Australian Bureau of Meteorology to improve the quality of the Geostationary AMVs. NESDIS has plans to test a new tracking algorithm which will improve the quality of the cloud drift winds derived from infrared window images (Daniels and Bresky 2010). Work also continues at the Australian Bureau of Meteorology to improve the quality of the H_2O technique (Le Marshall, 2010 personal communication) and to continue to develop quality control techniques using the Expected Error (EE) (Le Marshall et al. 2004).

REFERENCES

Daniels, J. and W. Bresky, 2010: A Nested Tracking Approach for Reducing the Slow Speed Bias Associated with Atmospheric Motion Vectors (AMVs). *10th International Winds Workshop,* Tokyo, Japan, 22-26 February 2010.

Hayden, C. M., and S. J. Nieman, 1996: A primer for tuning the automated quality control system for the verifying satellite-measured drift winds. NOAA Tech. Memo. NESDIS 43, 27pp.

Le Marshall, J., N. Pescod, R.Seaman, G. Mills, and P. Stewart, 1994: An Operational System for Generating Cloud Drift Winds in the Australian Region and Their Impact on Numerical Weather Prediction. *Wea. Forecasting*, **9**, 361-370.

__________, A. Rea, L. Leslie, R. Seecamp, and M. Dunn, 2004: Error characterization of atmospheric motion vectors., *Aust. Met. Mag.*, **53**, 123-131.

Menzel, W. P., W. L. Smith and T. R. Stewart, 1983: Improved cloud motion wind vector and altitude assignment using VAS. *J. Climate Appl. Meteor*., **22**, 377-384.

Nieman, S. J., J. Schmetz and W. P. Menzel, 1993: A comparison of several techniques to assign heights to cloud tracers. *J. Appl. Meteor*., **32**, 1559-1568.

Nieman, S. J., W. P. Menzel, C. Hayden, D. Gray, S. Wanzong, C. Velden and J. Daniels, 1997: Fully Automated Cloud-Drift Winds in NESDIS Operations. *Bull. Amer. Meteor. Soc*., **78**, 1121-1133.

Szejwach, G., 1982: Determination of semi-transparent cirrus cloud temperature from infrared radiances: Application to Meteosat. *J. Appl Meteor*., **21**, 384-393.

Su, X., J. Derber, D. Carlis, and R. Treadon, 2010: Improve Usage of Satellite Winds in the NCEP Data Assimilation System. *10th International Winds Workshop,* Tokyo, Japan, 22-26 February 2010.

APPENDIX

Deriving wind direction statistics:

Compute unit vectors from U and V for the observation and the model.

$$X_{ob} = U_{ob} \Big/ \sqrt{U_{ob}^2 + V_{ob}^2} \qquad Y_{ob} = V_{ob} \Big/ \sqrt{U_{ob}^2 + V_{ob}^2}$$

$$X_{mod} = U_{mod} \Big/ \sqrt{U_{mod}^2 + V_{mod}^2} \qquad Y_{mod} = V_{mod} \Big/ \sqrt{U_{mod}^2 + V_{mod}^2}$$

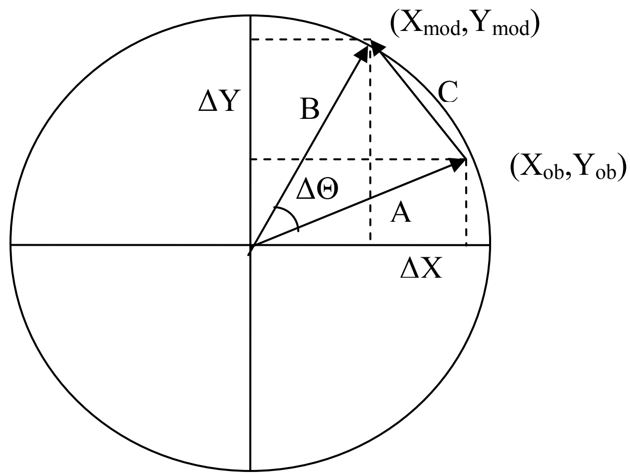

From the law of cosines, the angle between the observation and the model ($\Delta\Theta$) is given as:

$$C^2 = A^2 + B^2 - 2AB\cos(\Delta\Theta)$$

From the unit vectors:

$$A = B = 1$$

$$C^2 = 1 + 1 - 2\cos(\Delta\Theta)$$

Note:

$$C^2 = \Delta X^2 + \Delta Y^2$$

C is a scalar, direction can not be determined.

$$\Delta\Theta = ACOS\left(1 - C^2/2\right)$$

To determine direction, setup orthogonal vectors from (X_{ob}, Y_{ob}) and determine distance from (X_{mod}, Y_{mod}) to each orthogonal vector (Y_{ob}, $-X_{ob}$) and ($-Y_{ob}$, X_{ob}).

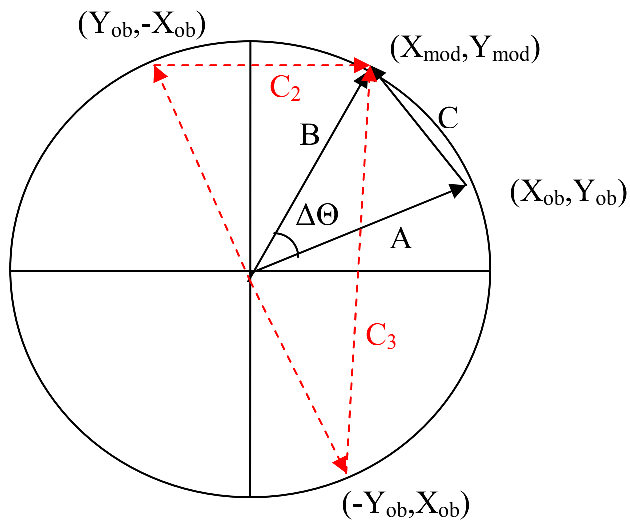

If $C_2 < C_3$, direction is counter-clockwise
If $C_2 > C_3$, direction is clockwise.

$$C_2^2 = (X_{mod} - Y_{ob})^2 + (Y_{mod} + X_{ob})^2$$

$$C_3^2 = (X_{mod} + Y_{ob})^2 + (Y_{mod} - X_{ob})^2$$

Expanding: $C_2^2 <=> C_3^2$ and canceling like terms

$$-X_{mod} Y_{ob} + Y_{mod} X_{ob} <=> X_{mod} Y_{ob} - Y_{mod} X_{ob}$$

So

$X_{ob} Y_{mod} < X_{mod} Y_{ob}$ counter-clocwise

$X_{ob} Y_{mod} > X_{mod} Y_{ob}$ clockwise